Scientific paper

Applications of Electron Probe Microanalyzer for Measurement of Cl Concentration Profile in Concrete

Daisuke Mori[1], Kazuo Yamada[2], Yoshifumi Hosokawa[3] and Masayoshi Yamamoto[4]

Received 2 July 2006, accepted 8 September 2006

Abstract

Electron probe microanalysis (EPMA) has been applied for the quantitative evaluation of Cl ingress into concrete. In order to obtain quantitative data on Cl concentration, the measurement conditions were discussed statistically in detail and sample measurement conditions were introduced. The absolute concentrations of Cl obtained through EPMA were found to be equivalent with wet analysis and the effect of matrix differences to be negligible. By using the difference in chemical composition between cement paste and aggregate measured by EPMA with a spatial resolution of 100 μm, it was possible to discriminate the paste part in concrete. Since Cl penetrates into concrete through the paste part, the Cl concentration profile obtained by EPMA is useful for the estimation of the apparent Cl diffusion coefficient, D_a. The quantified value of Cl concentrations obtained with EPMA were confirmed through comparison with traditional slicing and grinding methods. Based on the measurement results, the D_a value was calculated for various concrete mixtures and the results were found to be equivalent with those yielded by conventional methods.

1. Introduction

Electron probe microanalysis (EPMA) is an analysis method that allows the quantification of elemental concentrations with high spatial resolution and sensitivity on a solid surface as well as the measurement of the area distribution of elements. An apparatus with 4 or 5 spectrometers of the wavelength disperse type (WDS) is typically used these days for the simultaneous analysis of several elements. The element distribution measurement results are displayed as colored map images using a color scale, giving users an excellent visual grasp of element distribution.

EPMA was developed mainly for the fields of metallurgy and petrography. The first application of color mapping in the field of concrete technology was a study by Kobayashi *et al.* (1988-1, 1988-2) displaying the movement and accumulation of sodium and chloride ions by carbonation at the carbonation front. From this first application of color mapping, EPMA has been used effectively for various purposes related in particular to the durability of concrete such as the distribution of chloride and sulfur (Kawahigashi *et al.* 1992), chemical corrosion by sulfate (Sasaki *et al.*1994), leaching of calcium (Saito *et al.*1996), and chloride penetration through cracks (Win *et al.*2004). Recently, to allow the precise estimation of material transport, complex advanced models considering the material transport of various elements have been developed (for example, Tang and Nilsson 1997, Bentz and Garboczi 2001, Maekawa and Ishida 2001). As EPMA offers a high degree of spatial resolution for various elements, it is expected to be an effective tool for verifying complex advanced models for material transport in concrete (Johannesson *et al.*2005).

When EPMA began being used in the field of concrete technology, only color map images were available. However, rising computing power availability has made it possible to use numerical data obtained by EPMA in many ways. For example, the chloride concentration in the objective area was calculated by averaging the numerical data of corresponding pixels (Kawahigashi *et al.* 1991) or a chloride concentration profile was obtained from area analysis (Shiraki *et al.* 1990 for normal concrete, Jensen *et al.* 1999 for paste, Mori *et al.* 2002 for ultra-high strength concrete). Because the quality of the quantification by EPMA depends on the sample preparation and measurement procedure, in order to improve versatility and reproducibility, a committee within the Japan Society of Civil Engineers (JSCE) established a standard, JSCE-G574-2005, specifying sample preparation, measurement procedure, and numerical calculation of measured results (JSCE Standard 2005-1, JSCE 2006). In addition, standardization of EPMA is now under discussion by ISO/TC202. This paper discusses special requirements for the analysis of concrete, based on the average level of devices.

As basic data for the JSCE standard, the authors have developed a method for estimating the chloride diffusion coefficient based on a chloride profile measured by EPMA (Hosokawa *et al.* 2004). The spatial resolution of EPMA is better than that of conventional methods such as the slicing method (JSCE Standards 2004) and the grinding method (NORDTEST 1995, ASTM 2004). By using EPMA, a larger number of data points is available,

[1]R&D Center, Taiheiyo Cement Corp. Japan. (present: Research Center, Taiheiyo Consultant Co., Ltd.)
[2]R&D Center, Taiheiyo Cement Corp. Japan.
E-mail:kazuo_yamada@taiheiyo-cement.co.jp
[3]R&D Center, Taiheiyo Cement Corp. Japan.
[4]Research Center, Taiheiyo Consultant Co., Ltd. Japan.

thereby reducing apparent diffusion coefficient estimation errors. EPMA measurement of chloride concentration profiles is anticipated to present two problems. One is that the matrix effect on quantification is complex. Concrete being a porous material having various mixture proportions and different degrees of hydration, accurately quantified values are considered difficult to obtain. The other problem is uneven chloride concentration profiles having a spatial resolution of less than 1 mm owing to the arbitrary mixture of paste and aggregate. Moreover, the various measurement parameters may affect the measurement results.

Based on the above, to establish a measurement method of element concentration profiles with high spatial resolution, chlorine, Cl, were chosen as the investigation focus of this study because Cl ingress is one of the most important factors affecting the durability of concrete. The effectiveness of this method on concrete technology has been reported in a study on round robin testing carried out by a working group discussing the JSCE standard (Mori *et al.*2005). EPMA is used to evaluate total Cl content, which is composed of Cl ions in pore solution, chemically bound Cl in AFm phases such as Friedel's salt, and physically bound Cl in C-S-H. Only Cl ions in pore solution are expected to ingress into concrete. However, an apparent Cl diffusion coefficient, D_a, which is a coefficient describing the "apparent diffusion" of total Cl, is used to evaluate Cl ingress in many cases and Cl profiles obtained by EPMA are useful to estimate D_a. This paper mainly deals with the basic factors affecting the quantification results in greater detail based on previous studies (Yamada *et al.* 2004, Mori *et al.* 2004).

2. Outline of EPMA and subjects of investigation

2.1 EPMA

EPMA is an analytical method that uses an electron probe, in other words a convergent electron beam. The characteristic X-ray corresponding to the chemical composition of the sample is generated by the irradiation of the electron beam on a solid surface under vacuum. By analyzing the wavelength and intensity of the characteristic X-ray, it is possible to qualify and quantify the chemical composition of the sample at the location where the electron beam is irradiated. This is the basic principle of point analysis using EPMA.

The map image of an element can be obtained by scanning the sample with a fixed step width under a fixed electron beam, resulting in a map image of the element composed of pixels corresponding to the beam size. For example, using an electron beam with a diameter (probe diameter) of 100 μm, a step width of 100 μm, and a specimen size of 40 x 40 mm, a set of 400 x 400 pixels is obtained. The quantity of the objective element is initially expressed as an intensity of characteristic X-ray. The intensity of the X-ray is converted to mass% by using a calibration curve separately prepared based on standard samples. The concentration is expressed in a color scale and a 2D image of element distribution is obtained.

2.2 Key points of the investigation

As a nature of EPMA, only one cut surface is measured and this means that the results are affected by the uneven distribution of aggregate. In order to avoid the effect of aggregate, the paste was separated from the aggregate based on the differences in the chemical compositions of the paste and aggregate. Because Cl is expected to penetrate into concrete through the paste but not through the aggregate, this procedure is thought to be reasonable. Regarding the effect of the interfacial transitional zone (ITZ), one measurement indicated its existence by characteristic Cl penetration along coarse aggregate even in the case of ultra-high strength concrete when water suction occurred (Hosokawa *et al*. 2003). However, in ordinary concrete such as marine structures and in every concrete examined in this study, no preferential penetration along ITZ was observed (Sato *et al*. 2004).

Cl concentrations in the paste part were averaged along the same penetration depth from the concrete surface and used to make a Cl concentration profile. In order to obtain a sound profile representing the true concentration in concrete sample, the following three series of investigations were carried out. The factors and levels of investigation are listed in **Table 1**.

(1) Series 1: Quantitativity and measurement conditions

The characteristic X-ray generated by the irradiation of an electron beam being affected by the existence of a matrix (matrix effect), it is necessary to take into account the matrix effect for accurate quantification (Goldstein *et al.* 2003). The matrix effect includes the atomic number effect, X-ray absorption effect, and X-ray fluorescence effect caused by the different combinations of elements compared to standard materials. In cement paste, pore volume and existence of hydrates are expected to affect the matrix effect also. Therefore, in order to clarify the quantitativity of Cl, cement pastes having different concentrations of Cl were prepared and the results of measurement by EPMA and wet analysis as the standard were compared. The matrix effect of cement paste is expected to be caused also by differences in cement composition, W/C, and porosity related to the degree of hydration or age, and thus the effects of these factors were examined. The quantification accuracy was examined by changing the number of pixels averaged to obtain one data point to make a concentration profile. When the electron current density is too high, the sample is known to be damaged. For instance, Na and K in glass move from the surface of the sample toward the inside by irradiating the electron beam (JEOL 1983). Therefore, the effect of current density was examined by changing the probe diameter.

(2) Series 2: Discrimination of paste and aggregate

The discrimination of paste and aggregate was examined by using the differences between their chemical compositions, as listed in **Table 2**. Mortars having different sand/cement ratios (**Table 1**) were made in order to check the ability to discriminate between paste and aggregate. The differences in the CaO, SiO_2, and SO_3 contents of paste and aggregate were used for discrimination on a pixel by pixel basis. The effects of pixel size and probe diameter on the Cl concentration and the discriminating ability were also investigated.

(3) Series 3: Applicability for the evaluation of Cl diffusion in concrete

The measurement procedures optimized through Series 1 and 2 were applied for the evaluation of Cl diffusion in concrete immersed in a chloride solution. The measurement results by EPMA were compared with conventional methods and the repeatability and accuracy of the EPMA method were examined. From the measured Cl concentration profile, apparent diffusion coefficients were estimated and compared with those obtained by conventional methods.

3. Experiments

3.1 Materials and mixture proportion

Table 3 outlines the materials used in this study. The Cl concentration was adjusted by adding NaCl to the mixing water. The mixture proportions and general properties of concrete are shown in **Table 4**. For the examination of repeatability, concrete of 50N was used. Concrete slump was not controlled strictly but no material segregation

Table 1 Factors and levels of investigation.

Series	Investigated items	Factors	Levels[*1]
1	Quantitativity of Cl in paste, accuracy, detection limit, effects of types of cement	Cl concentration (C×%)	0, 0.5, 1.0, 2.0, 3.0, 4.0
		Types of cement	NPC (N), Slag blended cement type B (BB)[*3], Fly ash cement type B (FB)[*4]
	Pores in hardened body	W/B(%)	30, 40, 50
		Curing duration (days)	28, 91, 182
	Damage by electron beam	Probe diameter (μ m)	1, 5, 10, 25, 50, 100
2[*2]	Discrimination of paste	S/C	(0), 2.0, 3.0
	Pixel size, probe diameter	Pixel size (μ m)	10,25, 50, 100, 200
		Probe diameter (μ m)	The same with pixel size or 1/2 of it
3	Repeatability	Three samples were prepared from one concrete specimen. (n=3)	
	Verification in various concrete mixes	W/C(%)	30, 40, 50
		Types of cement	NPC, BB[*3], FB[*4]

*1) Underline indicates the level fixed to examine other factors. *2) Mortar used had W/C = 0.50 and Cl concentration = C×1.0 mass%. *3) Replacement ratio by slag was 40 mass%. *4) Replacement ratio by fly ash was 20 mass%.

Table 2 Examples of chemical compositions of cement paste and aggregate (mass%, JSCE 2005).

	Cement Paste *1	ISO sand	Sandstone	Hard sandstone	Siliceous rock	Limestone	Dolostone	Andesite	Basalt
CaO	46.4	0.20	5.50	5.65	—	53.44	33.10	5.80	8.95
SiO_2	15.1	98.4	78.33	65.05	98.87	1.97	1.30	59.59	49.06
SO_3	1.44	—	0.07	(S)0.05	—	—	—	—	—
Al_2O_3	3.72	0.4	4.77	13.89	0.41	0.78	0.45	17.31	15.70
Fe_2O_3	2.12	0.40	1.07	0.74	0.08	0.50		3.33	5.38

*1) Measured by XRF for paste having W/C = 0.50.

Table 3 Materials.

	Properties	Symbols	Series
Cement	Normal Portland cement (JIS R 5210, d = 3.16 g/cm^3)	N	1, 2, 3
Mineral admixture	Blast furnace slag (JIS A 6206, d = 2.85 g/cm^3, Blaine = 4000 cm^2/g)	B	1,3
	Fly ash (Type II by JIS A 6201, d = 2.06 g/cm^3)	FA	1,3
Fine agg.	ISO sand (d = 2.64 g/cm^3, SiO_2 = 98.4 mass%)	S1	2
	Land sand (d = 2.60 g/cm^3, absorption = 1.44 %)	S2	3
Coarse agg.	Crushed hard sandstone (G_{max} = 20 mm, d = 2.65 g/cm^3, absorption = 0.99 %)	G1	3 (30N, 40N, 50N)
	Crushed limestone (G_{max} = 20 mm, d = 2.70 g/cm^3, absorption = 0.74 %)	G2	3 (40FB, 40BB)
Chemical admixture	AE water reducer (Type I by JSI A 6204, Lignin sulfonate type)	AE1	3(40N, 50N, 40FB, 40BB)
	High range AE water reducer (Type I by JSI A 6204, Polycarboxylate type)	SP	3(30N)
	AE agent (Arkylallylsulfonate type)	AE2	3
Water	Distilled water	W1	1, 2
	City water	W2	3

Table 4 Mixture proportions of concrete.

Symbol	W/B (%)	s/a (%)	Unit content (kg/m^3)						Fresh properties		Compressive strength (N/mm^2)*1
			W (W2)	C (N)	FA	B	S2	G1 (G2)	SL. (cm)	Air (%)	
30N	30.0	46.0	160	533	0	0	749	889	24.0	3.5	90.5
40N	40.0	46.0	160	400	0	0	799	949	7.0	3.9	57.0
50N	50.0	46.0	160	320	0	0	830	985	9.0	3.7	46.6
40BB	40.0	46.0	160	240	0	160	793	(967)	10.0	4.3	50.0
40FB	40.0	46.0	160	320	80	0	783	(955)	8.0	4.5	47.2

*1) Cured at 20°C in water for 8 days.

was observed. Air content was in the range of 3.0 to 5.0%.

3.2 Preparation of specimens

The paste of Series 1 and the mortar of Series 2 were mixed in the amount of 1 liter using a mortar mixer with a 2 liter capacity. The mixtures were cast in a plastic container of 40 x 60 x 100 mm and sealed. At 1 day, the specimens were demolded and cured until 28 days of age in a moist condition. For one case in Series 1 checking the effect of age, the curing period was extended to 91 and 182 days. The concrete of Series 3 was mixed in the amount of 25 liters using a pan type forced-mixing mixer with a 50 liter capacity. For 50N, 40N, and 30N, concrete was cast in cylindrical molds of φ100 x H200 mm. For 40BB and 40FB, concrete was cast in rectangular molds of 100 x 100 x 400 mm. Specimens were demolded and cured in water at 20ºC until 28 days of age.

3.3 Immersion test in chloride solution

The immersion tests of concrete were carried out according to JSCE-G572-2003. For 50N and 30N, one surface of φ100 mm of a cylinder specimen was cut and exposed to a chloride solution. For 40N, the exposed surface was the mold surface. For 40BB and 40FB, 5 surfaces of a rectangular specimen were coated with epoxy resin and the specimens were exposed to a chloride solution. The condition of exposure was 3% NaCl solution at 20ºC for 91 days.

3.4 Analytical condition of EPMA

EPMA analysis was carried out basically according to JSCE-G574-2005 (JSCE 2005-1). The detailed procedure is explained in the literature (JSCE 2005-2). For Series 1 and 2, following moist curing, a specimen of 40 x 40 x 10 mm was sliced as a sample for EPMA measurement. The sliced specimen was reinforced by intrusion with epoxy resin not containing chlorine and ground to obtain a smooth surface. The ground sample was dried under vacuum and coated with carbon for EPMA analysis. The concrete of Series 3 was cut in parallel with the direction of Cl penetration from the immersion surface in a piece measuring 75 mm (W) x 30 mm (D) x 15 mm (H). The cut specimen was treated similarly to the samples of Series 1 and 2.

EPMA was done using 5 WDS detector channels to enable simultaneous measurement of Cl, Ca, Si, and S. The measurement conditions consisted in acceleration voltage of 15 kV, beam current of 100 nA, unit measurement time of 40 ms/point, pixel size of 100 μm, and probe diameter of 50 μm. In order to examine the damage caused by electron beam irradiation and the effect of pixel size and probe diameter, the pixel size and probe diameter were modified as shown in **Table 1**. The beam current for the examination of the damage caused by beam irradiation of Series 1 was set at 50 nA. Halite for Cl, wollastonite for Ca and Si, and anhydrite for S were used as the standard materials.

3.4 Cl concentration measurement by wet analysis

The specimens of Series 1 and 2 used for EPMA analysis were also used for wet analysis. The specimens were sliced perpendicular to the direction of Cl ingress and ground for Cl concentration measurement by acid dissolution and potentiometric titration according to JIS A 1154. Specimens of 30N, 40BB, and 40FB of Series 3 were ground with a milling machine from the exposed surface at 2 or 3 mm intervals and the ground powder was used for Cl concentration measurement by wet analysis to obtain Cl concentration profiles (grinding method). Specimens of 40N and 50N of Series 3 were sliced at 7 mm intervals (the first 3 mm from the surface were excluded) and Cl concentrations were measured by wet analysis according to JSCE-G572-2003 to obtain Cl concentration profiles (slicing method). The aggregate contents of the powders obtained with the grinding and slicing methods were estimated by measuring insoluble content according to the F-18 method of the Japan Cement Association and NDIS 3422 using sodium gluconate.

4. Results and discussions

4.1 Series 1: Quantitativity and measurement conditions

(1) Quantitativity of Cl concentration in cement paste

An example of area analysis by EPMA (400 x 400 pixels) is shown in **Fig. 1**. All the measured values of Cl concentration by EPMA are averaged and plotted against the values obtained through wet analysis in **Fig. 2**. The Cl concentration obtained through EPMA was converted from the intensity of the characteristic X-ray to mass

concentration of paste with a calibration curve using halite as the standard. The effect of density difference between paste and halite on Cl concentration was calibrated.

The measurement results obtained through EPMA show excellent linear correlation with the results obtained through wet analysis. For Cl, matrix effects on quantification by EPMA are found to be negligible. In general, the calibration of Cl concentration by EPMA should be based on the calibration curve between the intensity of the characteristic X-ray and the Cl concentration by wet analysis, as illustrated in **Fig. 5**. However, it is fortunate that when the Cl concentration of cement paste is calibrated using halite as the standard, the effect of the matrix on quantification is limited and it is easy and practical to use halite as a standard for quantification.

(2) Effect of matrix

Figure 2 shows the measurement results of BB and FB as well as N. There is a linear correlation between measurement results obtained through EPMA and wet analysis regardless of the type of cement. This indicates that the effect of the matrix through differences in the composition of cement is negligible. The effects of the water to binder ratio (W/B) and curing period on the measurement results of Cl concentration by EPMA and wet analysis are shown in **Figs. 3** and **4**, respectively. The general trend of the effects of W/C and curing period on the measurement results by EPMA is the same as that of wet analysis. Therefore, the quantification of Cl by EPMA using halite as the standard is judged accurate enough without special consideration of the mix proportion and curing period. When the chemical composition of the cement or microstructure differs significantly, a similar examination may be required.

(3) Detection limit of Cl concentration

Generally, concrete contains some Cl and this Cl concentration is express as C_0 and used for the estimation of D_a as explained in JSCE-G572-2003. Therefore, it is important to clarify the Cl detection limit by EPMA. In this study, the source of Cl in concrete is assumed to solely be the cement. Assuming Cl content of cement to be 0.007 mass% and W/B in a range of 0.30 to 0.50, C_0 is approximately 0.005 mass%.

In the case of point analysis by EPMA, in order to detect a minor element with a reliability of 99.7%, the net count rate, $N_P - N_B$, which is the difference between the count rate of the characteristic X-ray N_P and background N_B, should be more than three times standard deviation σ of $N_P - N_B$, as indicated by Eq. 1 (JEOL 1983-2).

$$N_P - N_B > 3\sigma \quad (1)$$

where N_P = gross count rate and N_B = count rate of background.

The variance V of $N_P - N_B$ is calculated by Eq. (2).

$$V = N_P + N_B \quad (2)$$

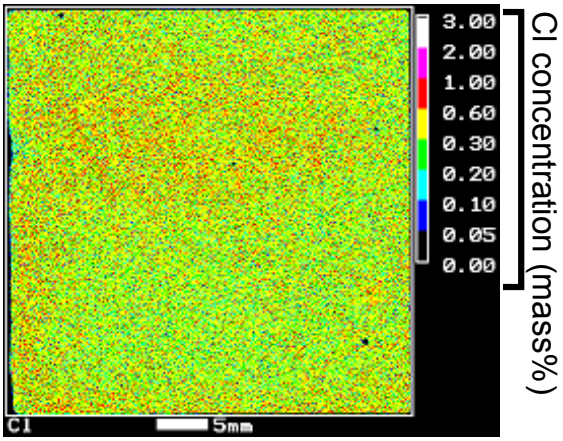

Fig. 1 Example of area analysis by EPMA (Paste, W/C = 0.50, Cl = 0.5 mass%-cement).

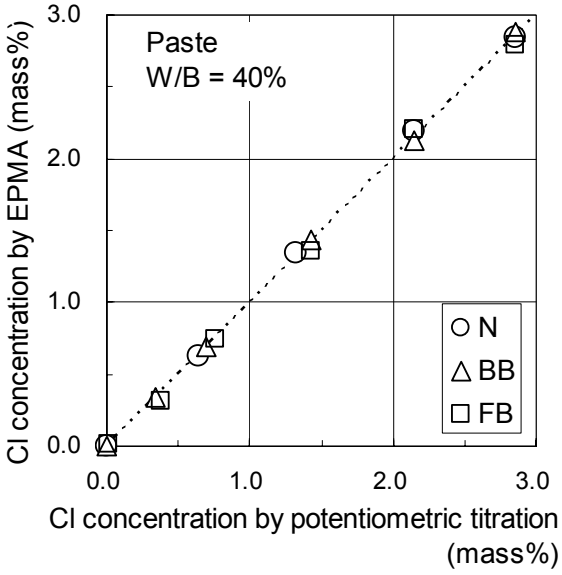

Fig. 2 Cl concentrations by EPMA and wet analysis.

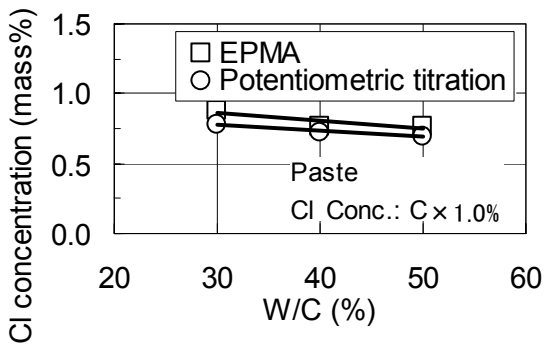

Fig. 3 Effect of W/C on Cl concentration.

For minor elements, it is possible to assume $N_P \fallingdotseq N_B$, and V is transformed to Eq. (3).

$$V = 2N_B \tag{3}$$

Based on the measurement results of Cl concentration in the range of 0 to 1.0 mass%-cement shown in **Fig. 2**, the count rate of the characteristic X-ray, which is an average value of 400 x 400 pixels, is plotted against the Cl concentration obtained through wet analysis. This relationship is shown in **Fig. 5**. The count rate in **Fig. 5** is normalized to the current value of 100 nA *i.e.* the value of the measured count rate divided by the measured current and multiplied by 100 nA. When the added amount of Cl is 0 mass%-cement, count rate N_P was 5.57, 5.86, and 6.14 for N, BB, and FB, respectively. The count rates of background N_B obtained from the intercept to the y axis of linear regression lines in **Fig. 5** were 5.22, 5.57, and 5.84 for N, BB, and FB, respectively. From these data, $N_P - N_B$ corresponding to the count rates of the characteristic X-ray of Cl concentration C_0 were 0.35, 0.29, and 0.30 for N, BB, and FB, respectively. The condition where $N_P - N_B$ is larger than the detection limit is discussed in the following section.

When the Cl concentration profile is made with the EPMA method, by averaging the Cl concentrations of pixels at the same depth, one representative value of Cl concentration at that depth is used. The number of pixels in this procedure is assumed as n. When variance V of the concentration of n pixels is known, the interval estimation of average μ is described by Eq. (4) using t-distribution.

$$\mu = \bar{x} \pm t \cdot \sqrt{\frac{V}{n}} \tag{4}$$

where $\bar{x}$ = Sample average.

Assuming one side of 99.7% confidence interval as α, α is described by Eq. (5).

$$\alpha = t(n-1, 0.03) \cdot \sqrt{\frac{V}{n}} \tag{5}$$

By using Eq. (1), the judgment equation is described as Eq. (6).

$$N_P - N_B > t(n-1, 0.03) \cdot \sqrt{\frac{V}{n}} \tag{6}$$

α depends on n, and the left-hand side of Eq. (6) is known through experiments. The minimum number of pixels used for averaging can thus be obtained. The relationship between pixel number n used for averaging and α is shown in **Fig. 6**. When n increases, the value of α and the detection limit decrease. The minimum numbers of pixels n satisfying Eq. (6) are 767, 1137, and 1116 for N, BB, and FB, respectively. Assuming the measurement width of an EPMA sample perpendicular to the direction of Cl ingress as 75 mm, the pixel size as 100 μm, the interval of Cl concentration profile in the paste part as 1 mm, and the ratio of the paste part to total pixels as 17%, the number of pixels existing in a 1 mm interval in the paste part is 1275, the corresponding value of α is 0.27, and the detection limit becomes lower than C_0 of 0.005 mass%.

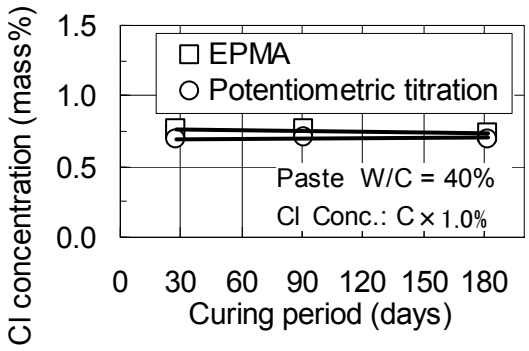

Fig. 4 Effect of curing period on Cl concentration.

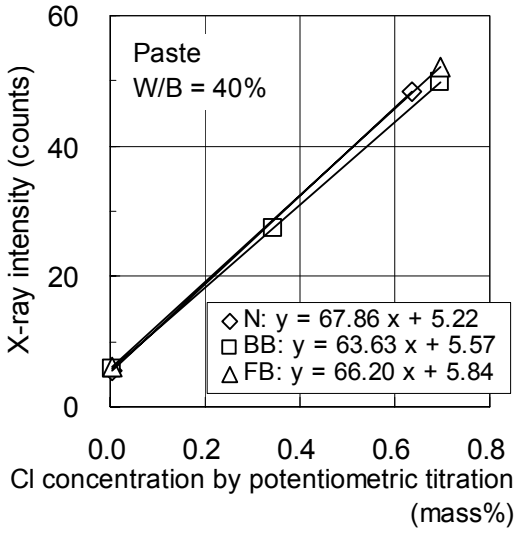

Fig. 5 Cl concentration and count rate of characteristic X-ray.

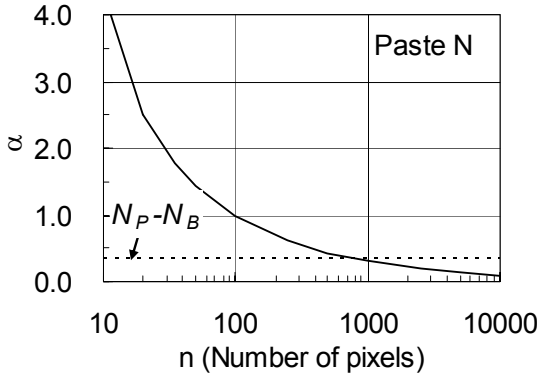

Fig. 6 Pixel number n and α (one side of 99.7 confidence interval).

(4) Accuracy of quantification of Cl concentration

As known from the color mapping of **Fig. 1**, the distribution of the Cl concentration in paste is inhomogeneous. The standard deviation of Cl concentrations of all pixels of sample N is plotted against the Cl concentration as shown in **Fig. 7**. The standard deviation of measured values increases with increases in Cl concentration. The coefficient of variation was calculated from **Fig. 7** and is shown in **Fig. 8**. Except the point around 0 mass% of Cl concentration, the coefficient of variation is approximately 30% and the Cl concentration of pixels used for averaging can be considered constant when it is expressed as a relative ratio. The reason of the large coefficient of variation around 0 mass% may be caused by background variations.

One side of the 95% confidence interval with 30% coefficient of variation is expressed by the relative percentage against the average value of Cl concentration (relative error), as shown in **Fig. 9**. It can be seen in that figure that the relative error decreases as the number of pixels increases and it becomes less than several % for pixel numbers greater than 750. This indicates that the accuracy of quantification of one pixel is low because of the short unit measurement time, but increasing the number of pixels for averaging yields the same improvement effect on quantification accuracy as increasing the measurement time. The relationship between the Cl concentration and estimated absolute error based on the coefficient of variation in **Fig. 9** was calculated for the averaged numbers of pixels of 750 and 1500 and is shown in **Fig. 10**. The absolute error increases with increases in Cl concentration. For example, the absolute error of Cl concentration is estimated as 0.022 mass% when the Cl concentration is 1.0 mass% and the number of pixels is 750. This level of accuracy is considered high enough to make a Cl concentration profile in concrete.

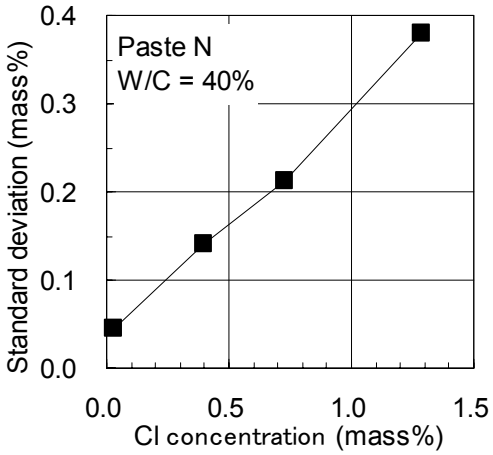

Fig. 7 Standard deviation of all pixels at each Cl concentration.

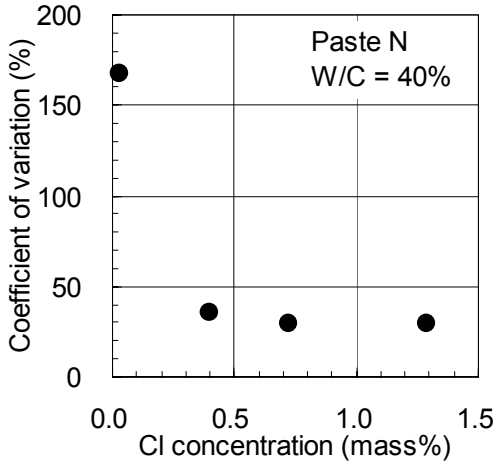

Fig. 8 Coefficient of variation of all pixels at different Cl concentrations.

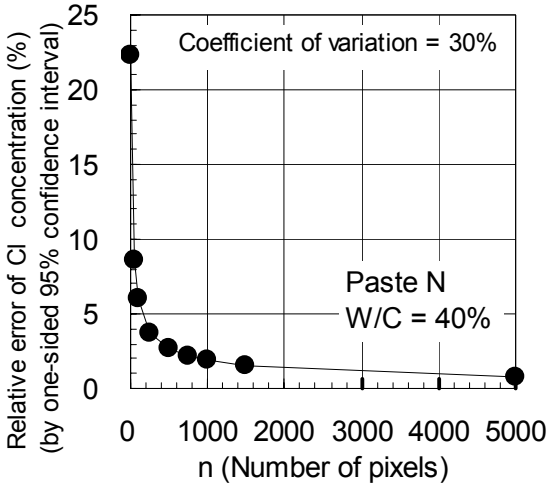

Fig. 9 Number of pixels and relative error of Cl concentration.

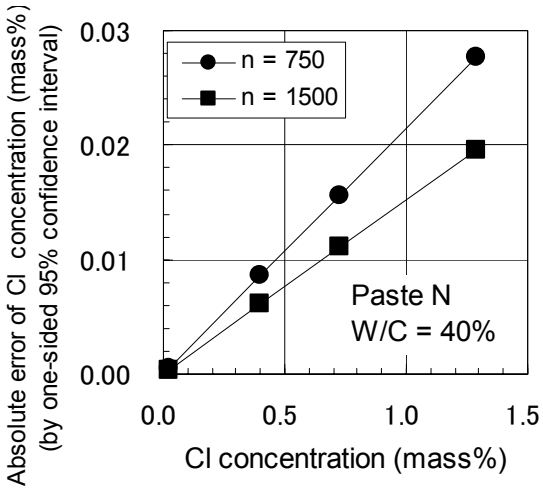

Fig. 10 Cl concentration and absolute error.

(5) Effect of measurement conditions on sample damage by electron beam irradiation

The Cl distribution in N cement paste was measured with a high spatial resolution and is shown in **Fig. 11**. When the pixel size was 0.5 μm, Cl concentration locations less than 10 μm in diameter were detected. These locations of high Cl concentration are estimated as Friedel's salt ($3CaO \cdot Al_2O_3 \cdot CaCl_2 \cdot 10H_2O$) based on the data of other elements such as Al and S that were measured simultaneously.

The variation in the relative count rate of the characteristic X-ray with time when the electron beam continuously irradiates the same position of high Cl concentration shown as white points in **Fig. 11** was measured and is shown in **Fig. 12**. When the probe diameter was larger than the area of Cl concentration, the centers of the probe and Cl concentrated area were set at the same position. As shown in **Fig. 12**, a smaller probe with higher current density showed a larger decrease in the relative count rate. When the probe size was 1 to 25 μm, a significant decrease in count rate was detected after 1 s of irradiation. This indicates the necessity of paying attention to the beam diameter, the beam current, and the measurement time at one pixel. When the beam size was larger than 50 μm and the beam current was 50nA, the current density was sufficiently low and no decreasing tendency in the count rate was detected, indicating the feasibility of stable analysis of Cl concentrations regardless of the current density and unit measurement time.

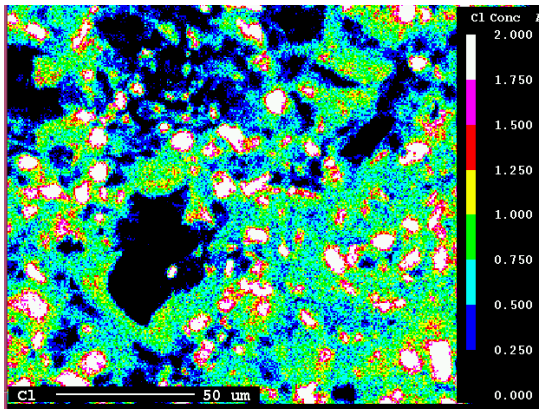

Fig. 11 Cl distribution in paste (pixel size = 0.5 μm).

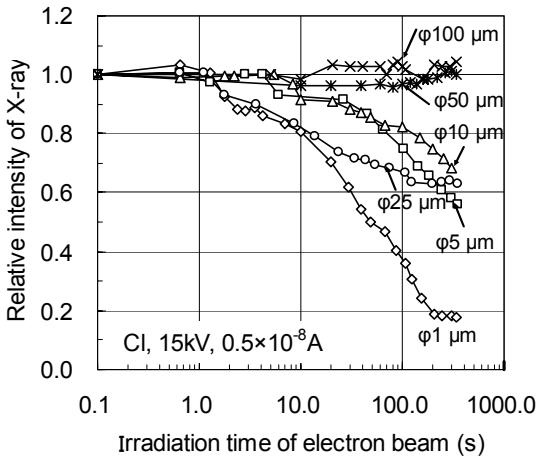

Fig. 12 Count rate change by electron beam irradiation.

4.2 Series 2: Discrimination of paste and aggregate

(1) Discrimination method

An example of area analysis by EPMA (400 x 400 pixels) of mortar is shown in **Fig. 13**. Scattered diagrams of concentrations of CaO and SiO_2 of mortar with S/C = 2.0 and paste with S/C = 0 are shown in **Fig. 14**. As shown in **Table 2**, ISO sand having a chemical composition of SiO_2 = 98.4 mass% and paste having a chemical composition of SiO_2 = 15.1 mass% and CaO = 46.4 mass%, there is a clear difference between their respective chemical compositions. The difference in chemical composition is also clear in the scattered areas of paste and aggregate in mortar, as shown in **Fig. 14**. The points between the paste and aggregate parts are considered as pixels that contain both paste and aggregate. The points having a lower CaO concentration are considered as a mixture with voids in one pixel. From this measurement, the range of cement paste is expressed as 18 mass% < CaO < 68 mass% and 2 mass% < SiO_2 < 28 mass%. Moreover, SO_3 being an element included only in paste but not in aggregate, it is effective for the discrimination between paste and aggregate. Based on the histogram of SO_3 concentration, the range of cement paste was 0.5 mass% < SO_3 < 6.25 mass%.

The average values of Cl concentration in the paste part of mortars having different S/C were plotted against

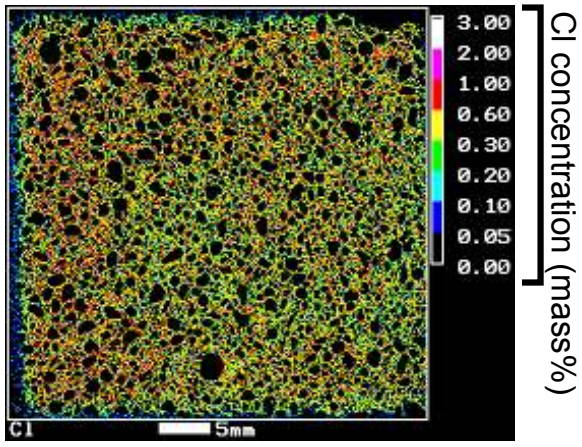

Fig. 13 Area analysis of Cl in mortar by EPMA (W/C = 0.50, S/C = 3.0, Cl = 1.0 mass%-cement).

S/C, are shown in **Fig. 15**. The Cl concentration was 1.0 mass%-cement and W/C was 0.50. Paste was discrimi-

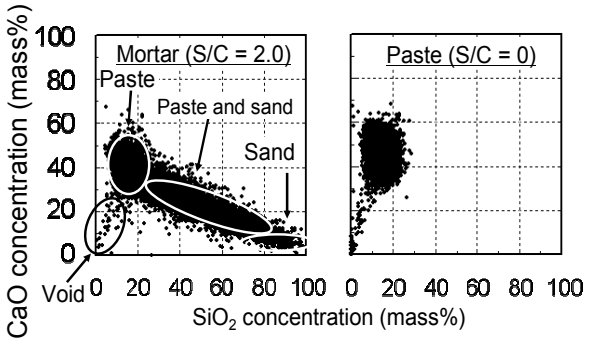

Fig. 14 Scatter diagram of CaO and SiO_2 for mortar and paste.

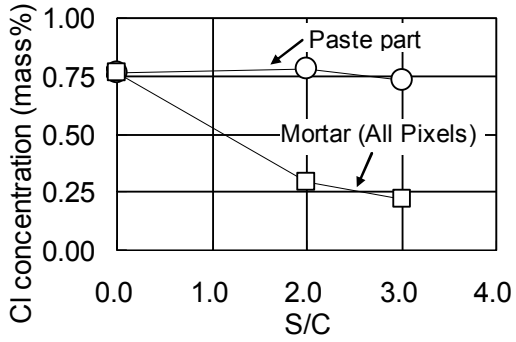

Fig. 15 Estimation of Cl concentration of paste in mortar.

nated by the difference in CaO, SiO_2, and SO_3 contents between paste and aggregate. The Cl concentrations in the paste part of mortars with S/C = 2.0 and 3.0 were equivalent with the Cl concentration in paste with S/C = 0. This indicates successful discrimination of the paste part using this procedure.

(2) Effects of pixel size and probe diameter on the Cl concentration

The relationship between the pixel size and the Cl concentration is shown in **Fig. 16 (a)**. The relationship between the pixel size and the ratio discriminated as paste (discrimination ratio = pixel number recognized as paste/total number of pixels) is shown in **Fig. 16 (b)**. The relationship between the pixel size and absolute error of Cl concentration estimated from the 95% confidence interval is shown in **Fig. 16 (c)**.

Figure 16 (a) indicates that quantitativity is adequate in the pixel size range of 25 to 100 μm because the same Cl concentrations were obtained. The reason why higher Cl concentration was detected for the pixel size of 10 μm may be the further discrimination of fine pores. The reason why lower Cl concentration was detected for the pixel size of 200 μm may be the contamination of larger pores.

As shown in **Fig. 16 (b)**, the larger the pixel size that is used, the lower the ratio of pixels recognized as paste,

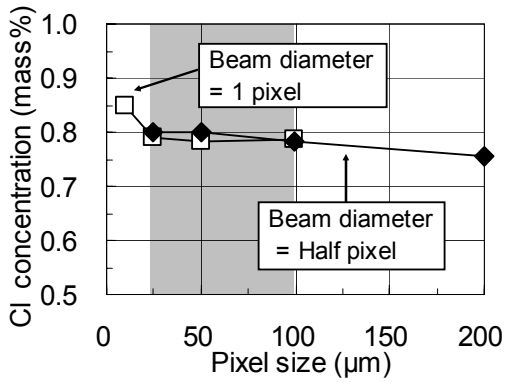

(a) Effect of pixel size on Cl concentration

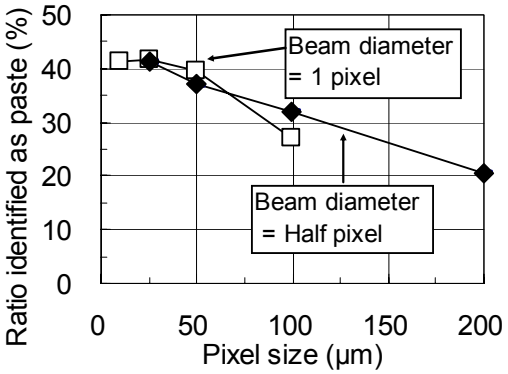

(b) Effect of pixel size on discrimination ability of paste

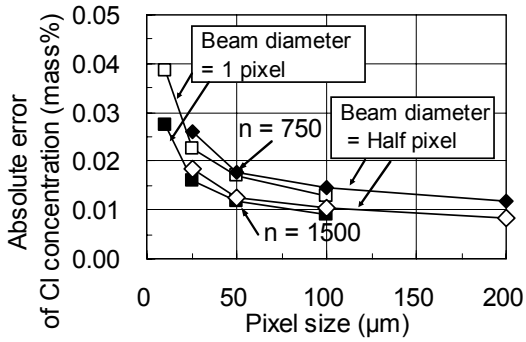

(c) Effect of pixel size on estimation error

Fig. 16 Effect of pixel size for the discrimination of paste part from mortar (W/C = 0.50, S/C = 2.0, Cl = 1.0 mass%-cement).

because the ratio of pixels containing both paste and aggregate increases. As shown in **Fig. 16 (c)**, the absolute error of Cl concentration decreases with increase in pixel size, and measurement with a pixel size larger than 50 μm can be recommend.

Based on the above, when measurement of the Cl concentration in the paste part is aimed for, from the viewpoints of quantitativity, discrimination of paste, and

absolute error, it is preferable to use a pixel size and probe diameter in the range of 50 to 100 μm. Comparing the cases when the probe diameter is the same as the pixel size and half the pixel size, no differences in the discrimination of paste part and quantitativity are seen.

4.3 Series 3: Applicability for the evaluation of Cl diffusion in concrete

(1) Repeatability

One example of area analysis by EPMA of the Cl concentration distribution in one of three concrete specimens of 50N is shown in **Fig. 17**. The Cl concentration profiles of three concrete specimens averaged at 1 mm intervals in the direction of Cl ingress are shown in **Fig. 18**. The Cl concentration profiles in the paste part were obtained using the method described in the section 3.2.

The Cl concentration profiles of concrete and in the paste part through EPMA method and the slicing method gave largely the same results and the accuracy of quantification by the EPMA method was confirmed again in concrete measurements. Deriving from the nature of EPMA measurement, the Cl concentration profiles on one cut surface of three different specimens of concrete showed significant differences whereas the slicing method showed high repeatability as shown in **Fig. 18(a)**. However, Cl penetrates into concrete through the paste part and EPMA can evaluate Cl movement in this paste part only. Therefore, it is only natural that reasonable repeatability was confirmed for the Cl concentration profiles of the paste part in concrete, as shown in **Fig. 18 (b)**. The coefficients of variation of the Cl concentration profiles of the three specimens, which is a total average of the coefficients of variation at each depth, are summarized in **Table 5**. The coefficient of variation of the Cl concentration profile in the paste part through the EPMA method is equivalent with that obtained with the conventional slicing method. The merit of the EPMA method is the high spatial resolution and much greater number of data points for the regression calculation to estimate D_a.

(2) Comparison of EPMA method with conventional methods

Examples of area analysis of the Cl concentration for various mixtures by EPMA are shown in **Fig. 19**. The Cl concentration profiles of each mixture obtained through EPMA are shown in **Fig. 20**, compared with the slicing and grinding methods. **Figure 20** shows that the quantitativity of EPMA is equivalent with that of other conventional methods.

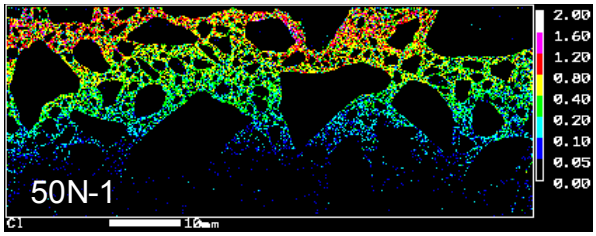

Fig. 17 Area analysis by EPMA for 50N-1.

Table 5 Comparison of repeatability of Cl concentration profiles by coefficients of variation (50N, n = 3).

	Concrete	Paste part
EPMA	22.8%	14.0%
Slicing	11.1%	12.5%

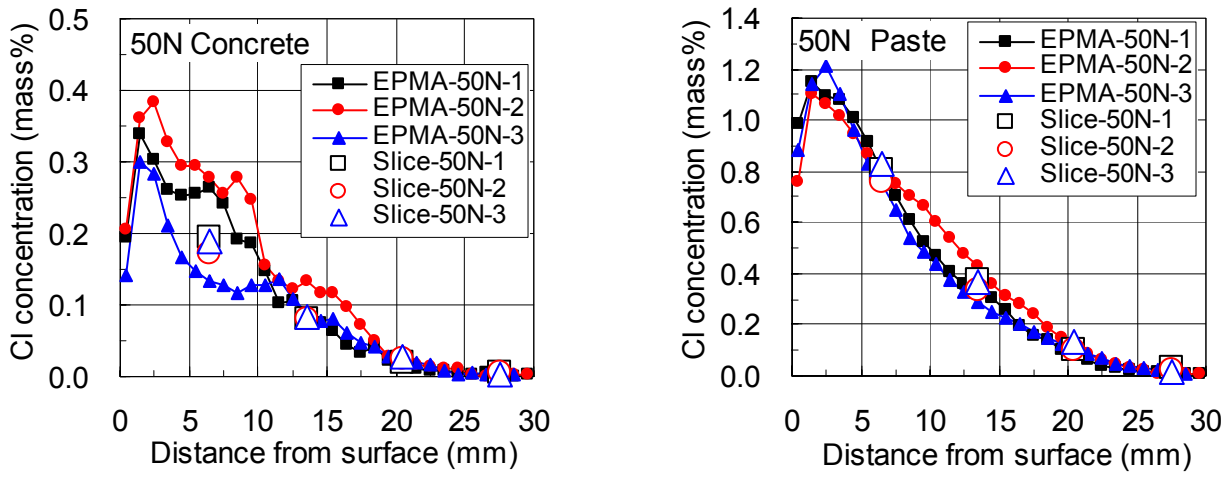

(a) Concrete (b) Paste

Fig. 18 Repeatability of Cl concentration profile by EPMA (50N, n = 3).

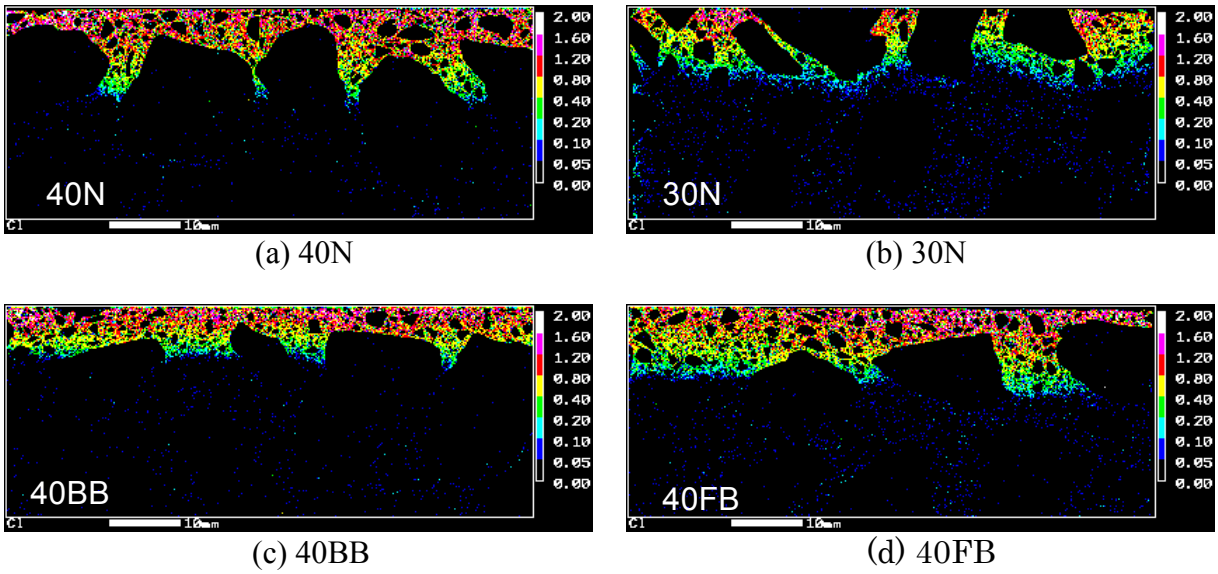

(a) 40N (b) 30N

(c) 40BB (d) 40FB

Fig. 19 Area analysis by EPMA.

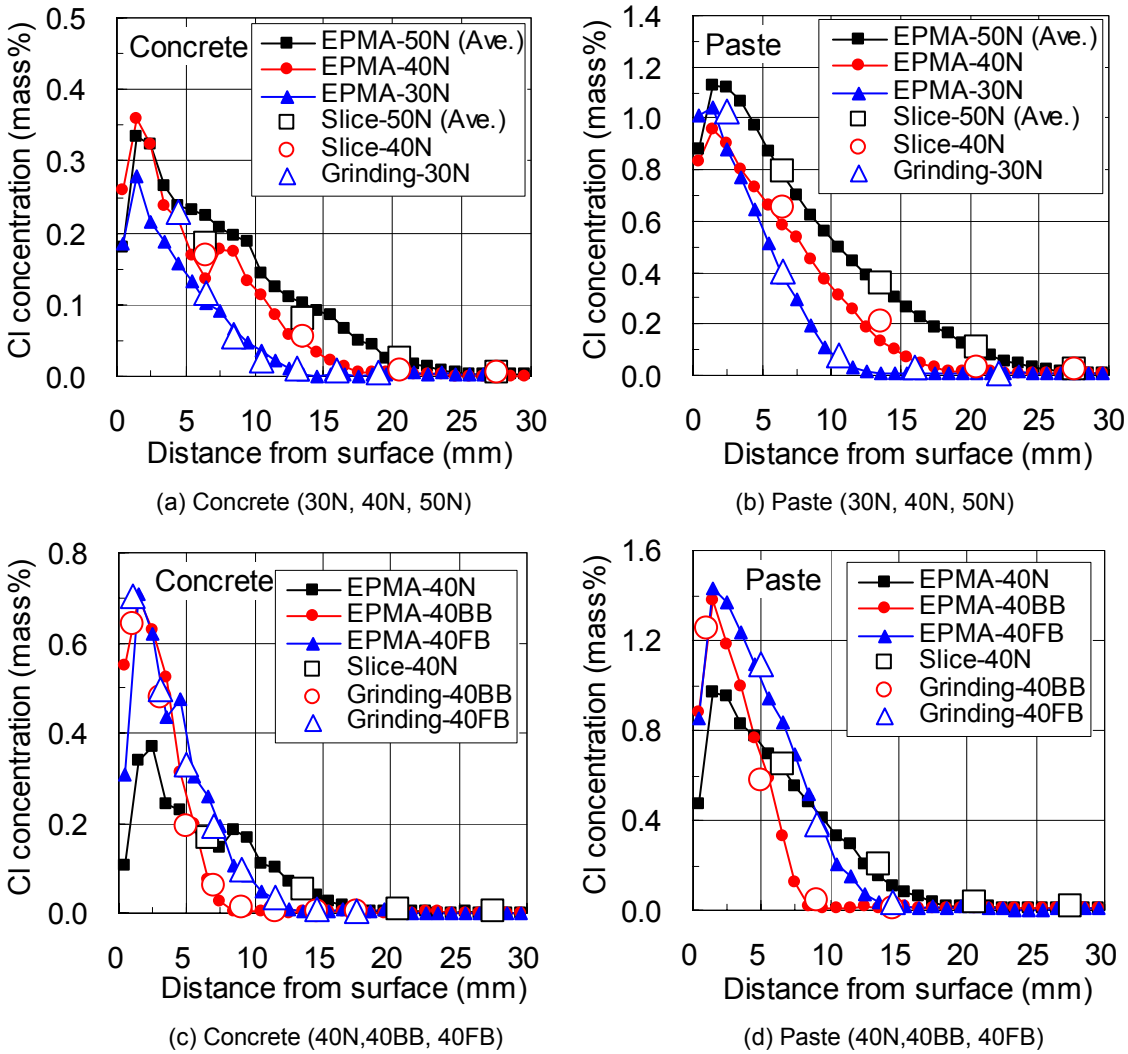

(a) Concrete (30N, 40N, 50N)

(b) Paste (30N, 40N, 50N)

(c) Concrete (40N,40BB, 40FB)

(d) Paste (40N,40BB, 40FB)

Fig. 20 Cl concentration profiles.

(3) Verification of the accuracy of quantification by EPMA in concrete

The detection limit and the accuracy of quantification were discussed for paste in section 4.1. Here, a similar discussion will be carried out for concrete, using a Cl concentration profile in the paste part of 40N concrete with 1 mm intervals. The total number of pixels in a 1 mm interval was 7500 and the average number of pixels judged as paste was 1130, with a standard deviation of 237.

The relationship between the count rate of the characteristic X-ray and the Cl concentration is shown in **Fig. 21 (a)**. The count rate corresponding to C_0 was 5.10 and the count rate corresponding to Cl = 0 mass% was 4.78, thus a difference of 0.32 between the two. The Cl concentration of C_0 was 0.0049 mass%. In order to detect the Cl concentration corresponding to the count rate of 0.32, the required number of pixels was 828. This number was obtained using the calculation explained in section 4.1 (3) and is equivalent with the required number of 767 pixels for detecting Cl = 0.005 mass% in paste discussed in section 4.1 (3).

The relationship between the average Cl concentration of pixels judged as paste and the coefficient of variation is shown in **Fig. 21 (b)** with the results of the paste shown in **Fig. 8**. The relationship between the Cl concentration and the absolute error is shown in **Fig. 21 (c)**. The relationships of concrete and paste are equivalent and these results indicate that the conclusion that 1000 pixels is a preferable number for accurate analysis in the discussion for the paste is confirmed in concrete again. In **Fig. 21 (c)**, at higher Cl concentrations than 0.75 mass%, the reason why the absolute error decreases lies in the greater number of pixels judged as paste with higher Cl concentrations than 0.75 mass%. As shown in **Fig. 19 (a)**, Cl penetrated from the mold surface and the extent of penetration was limited in the area having "wall effects." The paste content is richer near the mold surface and the portion of paste is greater than at deeper locations free from Cl penetration.

(4) Application for the estimation of D_a

The Cl concentration profiles shown in **Figs. 18** and **20** were used to estimate apparent Cl diffusion coefficients, D_a, by fitting to Fick's 2nd law. The calculation results are shown in **Fig. 22**. In general, equivalent results were obtained regardless of the use of different methods for measuring the Cl concentration profiles. The estimation errors are indicated by error bars in **Fig. 22**. The estimation errors of EPMA are relatively smaller than for other methods. Therefore, EPMA can be judged as an effective tool to estimate D_a.

Figure 23 shows the Cl concentration profiles reproduced by D_a and the measured data. The Cl concentration profiles obtained by each measurement method show a similar general trend. However, there are some differences in the Cl concentration at the surface. As shown in **Fig. 19**, the ratio of paste in concrete near the surface is

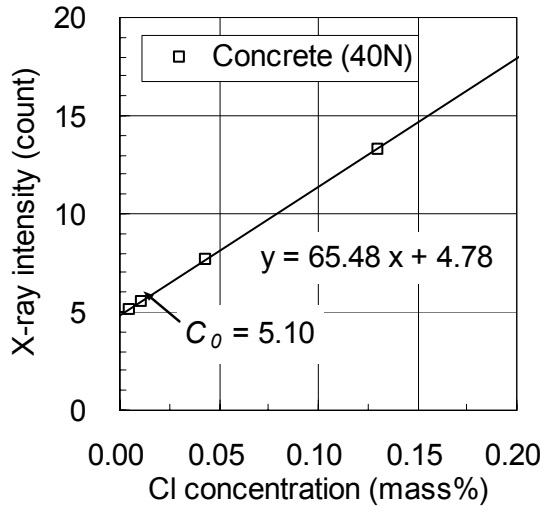

(a) Detection limit

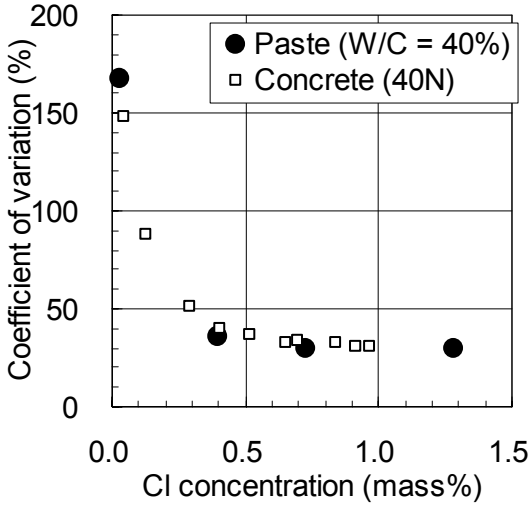

(b) Coefficient of variation of Cl concentration

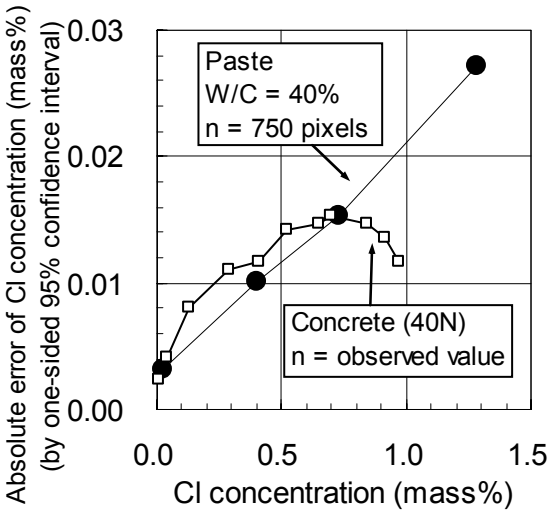

(c) Absolute error of Cl concentration

Fig. 21 Verification of accuracy of quantification of Cl concentration profile in concrete by EPMA.

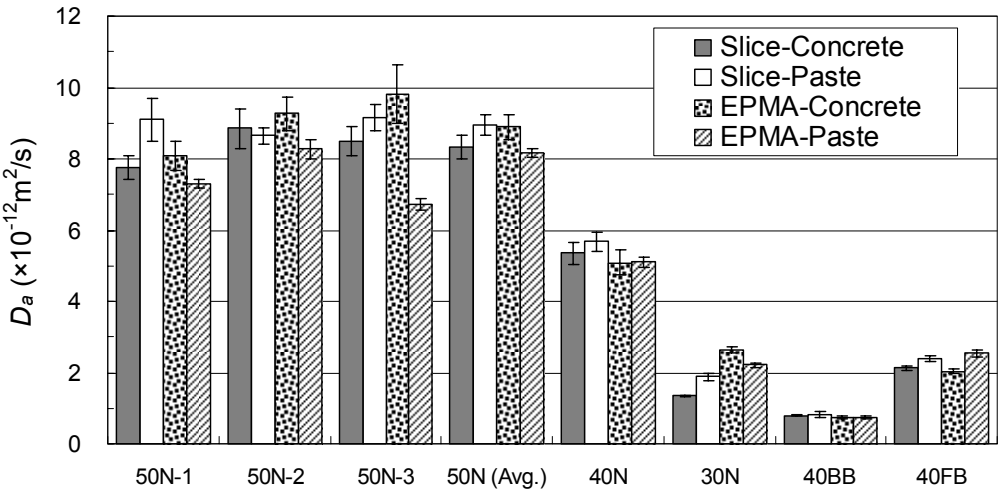

Fig. 22 Estimation of apparent Cl diffusion coefficient.

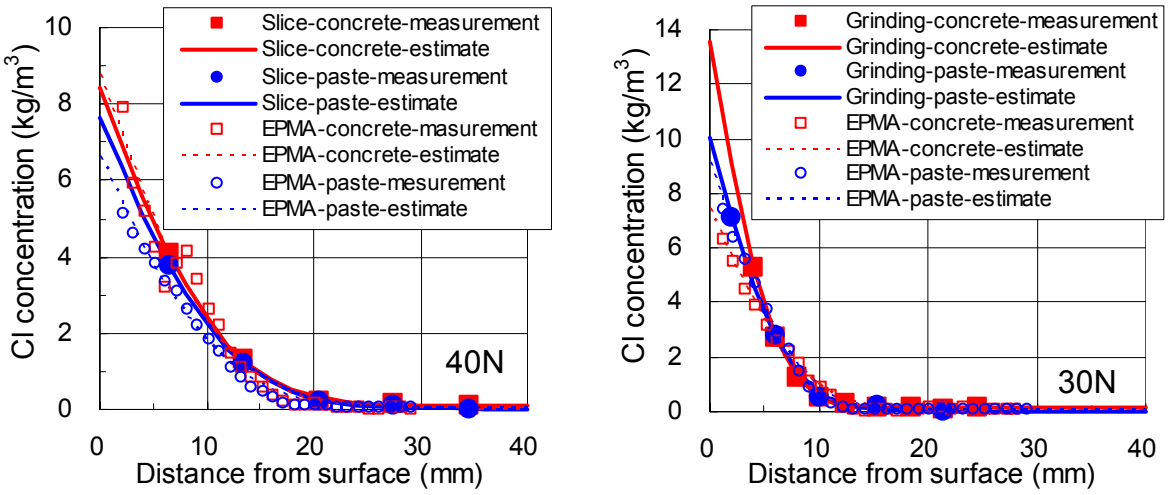

Fig. 23 Comparison of Cl concentration profiles reproduced by estimated D_a.

different depending of the nature of the surface (whether mold surface or cut surface). Cl penetrates only in the paste part. Therefore, the Cl concentration should be measured for the paste part and not for the concrete.

One more important fact is the decrease in Cl concentration near the surface as shown in **Figs. 18** and **20**. Based on EPMA measurement, there are Cl concentration peaks near the surface. This detailed distribution of Cl concentration seems difficult to detect with the slicing and grinding methods. Therefore, when slicing and grinding methods are used to estimate D_a, special attention should be paid for the Cl concentration data at the surface of the concrete exposed to the Cl solution.

5. Conclusions

The measurement of Cl concentration profiles by EPMA was studied and the following conclusions were obtained.

(1) Because Cl penetrates into concrete through the paste part, the quantitativity of the EPMA method for Cl concentration using paste samples was confirmed. The average values of all pixels obtained by area analysis of EPMA gave equivalent values by wet analysis. The effect of matrix differences in the cement paste was limited and the effect of the type of cement, W/C, and curing period was almost negligible.

(2) Based on the statistical discussions of a detection limit and quantification errors for Cl concentrations, the use of approximately 1000 pixels is recommended for averaging. When more than 750 pixels were used, it was possible to reduce the quantification relative error to less than several %.

(3) Regarding damage by electron beam irradiation, when the probe diameter is 1 to 25 μm, special at-

tention had to be paid to the beam current and unit measurement time because a decrease in the count rate of the characteristic X-ray of Cl was detected after 1 s of irradiation. When the probe diameter was set to a value larger than 50μm, the decrease in count rate was small and the effect of current density was negligible.

(4) Taking into account the difference in chemical composition between the paste part in concrete and aggregate, it was possible to discriminate between the pixels of paste and aggregate. From the viewpoints of quantitativity, discrimination of the paste part, and absolute error, the pixel size and probe diameter should preferably be set to approximately 50 to 100 μm.

(5) Cl concentration profiles were evaluated by EPMA with an interval of 1 mm for concrete immersed in a chloride solution. The Cl profiles obtained with the EPMA method for various concretes of different W/C and the types of cement matrix were identical with those obtained with conventional methods such as slicing and grinding methods.

(6) The accuracy of quantification by EPMA was examined by comparing the Cl concentration profiles in the paste part of three different specimens from the same concrete. The Cl concentration profiles were identical with those obtained with conventional methods. The EPMA method had accuracy equivalent with that yielded by the slicing and grinding methods.

(7) The apparent Cl diffusion coefficients were estimated from the Cl concentration profiles using the EPMA method. The estimated values were the same as those obtained using conventional methods such as the slicing and grinding methods. The data interval for the EPMA method was much smaller than traditional methods and the much higher number of data points was beneficial for reducing estimation errors for the apparent diffusion coefficients of Cl.

Acknowledgements

The authors wish to thank Ms. Haruka Takahashi of Taiheiyo Cement Corp. and Dr. Kazuo Yamamoto of Taiheiyo Consultant Co. Ltd for their significant contributions to the conduct of experiments and data processing for EPMA. Dr. Hideyuki Takahashi of JEOL is also gratefully acknowledged for his valuable comments on this study.

References

ASTM (2004). "Standard test method for determining the apparent chloride diffusion coefficient of cementitious mixtures by bulk diffusion." ASTM C 1556-04.

Awaya, R. (1991). "Analog and digital." Gakkai Syuppan Center, 32 and 52-53 (in Japanese).

Bentz, D. P. and Garboczi, E. J. (2001). "Multiscale microstructural modeling to predict chloride-ion diffusivity for high performance concrete." ed. Hooton, R. D., *et al*., *Materials Science of Concrete, Ion and Mass Transport in Cement-Based Materials*, The American Ceramic Society, 253-267.

Goldstein, J. I., editor. (2003). "Scanning electron microscopy and X-ray microanalysis." 3rd Edition, Kluwer Academic/Plenum Publishers, 403-421.

Hosokawa, Y., Yamada, K. and Yamamoto, M. (2003). "Evaluation of chloride penetration into ultra high strength concrete by using grinding and EPMA methods." *Proceedings of Annual Conference of AIJ*, 563-564 (in Japanese).

Hosokawa, Y., Yamada, K., Mori, D. and Kim, D. S. (2004). "Evaluation of chloride penetration into concrete using electron probe micro analysis." *Proceedings of the Fourth International Conference in Concrete under Severe Condition* (CONSEC 2004), 1, 867-872.

Jensen, O. M., Hansen, P. F., Coats, A. M. and Glasser, F. P. (1999). "Chloride ingress in cement paste and mortar." *Cement and Concrete Research*, 29, 1497-1504.

JEOL Training Center (1983). "Practical techniques for microprobe analysis." JEOL, 85-87.

JEOL Training Center (1983-2). "Practical techniques for microprobe analysis." JEOL, 81.

Johannesson, J., Yamada, K., Hosokawa, Y. and Mori, D. (2005). "An approach for the evaluation of combined process of chloride penetration and carbonation by a multi-species model." *Taiheiyo Cement Kenkyu Hokoku* (Journal of Research of the Taiheiyo Cement Corporation), 148, 4-11.

JSCE (2004). "JSCE STANDARDS, Test method for apparent diffusion coefficient of chloride ions in concrete by immersion in salt water (JSCE-G572-2003)." JSCE Standards on test method for diffusion coefficient of chloride ion concrete, JSCE (in Japanese).

JSCE STANDARDS (2005-1). "Area analysis method of elements distribution in concrete by using EPMA (JSCE-G574-2005)." *Concrete Engineering Series*, 69, 6-17 (in Japanese).

JSCE (2005-2). "Area analysis method of elements distribution in concrete by using EPMA (JSCE-G574-2005)." *Concrete Engineering Series*, 69, 64 (in Japanese).

JSCE (2005-3). Concrete Engineering Series, 55, 94-95 (in Japanese).

JSCE Sub-Committee on New Standards, Committee on Concrete (2006). "JSCE Standards, Area analysis method of elements distribution in concrete by using EPMA." *Journals of Materials, Concrete Structures and Pavements*, JSCE, 809/V-70, 1-14 (in Japanese).

Kawahigashi, T., Watanabe, Y., Inoue, S., Miyagawa, T. and Fujii, M. (1991). "Deterioration mechanism of salt damage/ carbonation of concrete." *Proceedings of Annual Conference of the Japan Society of Civil*

Engineers, 46, 322-323 (in Japanese).

Kawahigashi, T., Tamano, I., Fujii, M., Inoue, S. and Miyagawa, T. (1992). "Deterioration of concrete caused by combined factors of salt-damage/acid-corrosion." *Proceedings of Annual Conference of the Japan Society of Civil Engineers*, 47, 334-335 (in Japanese).

Kobayashi, K., Shiraki, R. and Masaki, T. (1998-1). "Concentration gradient of alkalis in concrete members—Analysis by electron probe micro-analyzer." *Seisan-Kenkyu* (Monthly Journal of Institute of Industrial Science, University of Tokyo), 40, 47-50 (in Japanese).

Kobayashi, K., Shiraki, R., Uno, Y. and Kawai, K. (1988-2). "Carbonation and concentration of chlorine in concrete containing chlorides (1)." *Seisan-Kenkyu* (Monthly Journal of Institute of Industrial Science, University of Tokyo), 40, 33-36 (in Japanese).

Maekawa, K. and Ishida, T. (2001), "Service-life evaluation of reinforced concrete under coupled forces and environmental actions." ed. Hooton, R. D., *et al*., *Materials Science of Concrete, Ion and Mass Transport in Cement-Based Materials*, The American Ceramic Society, 219-238.

Mori, D., Uzawa, M., Katagiri, M. and Shimoyama, Y. (2002). "Consideration by diffusion theory concerning chloride ion penetration of RPCM." *Proceedings of Annual Conference of the Japan Cement Association*, 56, 176-177 (in Japanese).

Mori, D., Hosokawa, Y., Yamada K. and Yamamoto, M. (2004). "Application of EPMA for the determination of chloride ion concentration profile in concrete." *Proceedings of the Japan Concrete Institute*, 26, 867-872 (in Japanese).

Mori, D., Yamada, K., Yamazaki, D., Takahashi, H. and Takewaka, K. (2005). "Area analysis of elements in concrete by EPMA method: Round robin test." *Proceedings of Annual Conference of JSCE*, 60, 531-532 (in Japanese).

NORDTEST (1995). "Concrete, hardened: Accelerated chloride penetration, NT BUILD 443." Eabo, Finland.

Saito, H., Nakane, S., Tajima, T. and Fukuhara, A. (1996). "Deterioration of cement hydrate by electrical acceleration test method." *Proceedings of the Japan Concrete Institute*, 18, 969-974 (in Japanese).

Sasaki, H., Taniguchi, K., Hironaga, M. and Endo, T. (1994). "Judgment of chemical corrosion of mortar caused by sulfate using EPMA." *Proceedings of the Japan Concrete Institute*, 16, 859-864 (in Japanese).

Sato, M., Hosokawa, Y., Mori, D., Johanneson, B. and Yamada, K. (2004). "Behavior analysis of various ions that migrate in marine structures and proposal of modeling." JCI-C64 (committee report), 293-300 (in Japanese)

Shiraki, R., Kawai, K. and Kobayashi, K. (1990). "Quantitative analysis of trace elements in hardened cement paste by EPMA." *Proceeding of the Japan Concrete Institute*, 12, 365-370 (in Japanese).

Tang, L. and Nilsson, L-O. (1997). "Accelerated tests for chloride diffusivity and their application in prediction of chloride penetration." *Mechanisms of Chemical Degradation of Cement-based Systems*, E & FN Spon, 387-396.

Win, P. P., Watanabe, M. and Machida, A. (2004). "Penetration profile of chloride ion in cracked concrete." *Cement and Concrete Research*, 34, 1073-1079.

Yamada, K., Mori, D., Hosokawa, Y. and Yamamoto, M. (2004). "Application of EPMA for the estimation of apparent diffusion coefficient of chloride ions in concrete." *Proceedings of Annual Conference of the Ceramic Society of Japan*, 124 (in Japanese).